

ON THE USE OF ENERGY DISPERSIVE X-RAY REFLECTION TO STUDY THE ELECTRONIC DENSITY PROFILE AT SURFACES AND INTERFACES

R. FELICI

Istituto di Struttura della Materia del C.N.R., Via E. Fermi 38, I-00044 Frascati, Italy

Introduction

Specular reflection of X-rays from surfaces and interfaces can be used to gain structural information in the Å region [1]. Simple specular reflection measurements allow us to determine the electronic density profile along the direction perpendicular to the reflecting surface or interface. The applications of this technique are then very wide and it has been used to study the structure of insoluble monolayer [2] and ions bound to them [3], and more recently to study the structure of a liquid-liquid interface [4].

X-ray reflectivity is usually measured using a monochromatic incident radiation as a function of the incidence angle. In this article we will show that this measurements can be also performed at fixed angles of incidence and by using an energy dispersive detector. We will discuss the main advantages of this method and outline the instrument that we have built and that is operational at our laboratory. We will also describe some of the measurements that we have recently performed.

Theory

The theory of the specular reflection of X-rays and of particle waves can be found elsewhere [5] and in this article we will only outline the basic principles. In an X-ray reflectivity experiment we measure the intensity as a function of the exchanged momentum \mathbf{Q} ($Q=4\pi/\lambda \sin(\mathbf{J})$) when a well collimated beam impinges onto a surface at grazing angle of incidence \mathbf{J} . For an X-ray beam the general complex expression of the refractive index of a medium is [6]:

$$n(z) = 1 - \frac{1^2}{2p} r_e(z) r_e + i \frac{1}{4p} m(z) \quad (1)$$

where λ is the incident radiation wavelength, r_e is the electronic density as a function of the distance

from the surface z , r_e is the classical electron radius and μ is the linear absorption coefficient. The quantity $\text{Per } e' \text{ scattering length density}$, is of the order of 10^{-5} \AA^{-2} ; the refractive index is therefore slightly smaller than one and total reflection occurs only at grazing angles of incidence. The imaginary component of the refractive index is responsible for the absorption. In general this term is of the order of 10^{-7} \AA^{-1} and is neglected in the calculation. This may not be true anymore when the energy of the beam is close to an absorption edge and the contribution of the imaginary part should be fully calculated.

Once we have defined the expression of the refractive index we can use all the formalism developed for classical optics and the reflectivity can be easily calculated as a function of the exchanged momentum. For instance in the simple case of a sharp interface between two media, denoted with 1 and 2, we can use the Fresnel formula:

$$R_0(Q) = \left| \frac{n_1(\mathbf{I}) \sin(\mathbf{J}_1) - n_2(\mathbf{I}) \sin(\mathbf{J}_2)}{n_1(\mathbf{I}) \sin(\mathbf{J}_1) + n_2(\mathbf{I}) \sin(\mathbf{J}_2)} \right|^2 \quad (2)$$

where \mathbf{J}_1 and \mathbf{J}_2 are the angles of the directions of the incident or reflected and of the transmitted beams with respect to the separation surface.

If the interface is not sharp and the variation of the scattering length density can be described by a normal distribution with respect to the distance from the interface, then the reflectivity is modified by a term similar to a DebyeWaller factor [7]: (3)

$$R(Q) = R_0(Q) \cdot \exp\left(-\frac{16p^2}{I^2} \sin(\mathbf{J}_1) \sin(\mathbf{J}_2) \langle s_{1,2} \rangle^2\right)$$

where R_0 is the ideal reflectivity, calculated using eq. (2), and $\sigma_{1,2}$, the surface roughness, is the dimension of the interface along the "z" direction.

In the general case, the refractive index profile is a complicated function of the distance from the

surface and to calculate the reflectivity we need to solve a system of integral equations [8]. Moreover, if the sample can be divided in a series of contiguous homogeneous layers, as for instance in a superlattice, it is more practical to use the matrix method [9]. In this case the transport properties of the “j” layer are described by a characteristic 2x2 matrix, M^j , whose components, in terms of the Fresnel reflectivity coefficients, are [10]:

$$\begin{aligned} M_{1,1}^j(\mathbf{I}, \mathbf{J}) &= \exp(i\mathbf{b}_j); \\ M_{2,2}^j(\mathbf{I}, \mathbf{J}) &= \exp(-i\mathbf{b}_j); \\ M_{1,2}^j(\mathbf{I}, \mathbf{J}) &= r_{j,(j+1)} \exp(i\mathbf{b}_j); \\ M_{2,1}^j(\mathbf{I}, \mathbf{J}) &= r_{j,(j+1)} \exp(i\mathbf{b}_j); \end{aligned} \quad (4)$$

where the $r_{j,(j+1)}$ terms are defined as:

$$\begin{aligned} r_{j,(j+1)} &= \frac{n_j(\mathbf{I}) \sin(\mathbf{J}_j) - n_{j+1}(\mathbf{I}) \sin(\mathbf{J}_{j+1})}{n_j(\mathbf{I}) \sin(\mathbf{J}_j) + n_{j+1}(\mathbf{I}) \sin(\mathbf{J}_{j+1})} \cdot \\ &\exp\left(-\frac{8p^2}{I^2} \sin(\mathbf{J}_j) \sin(\mathbf{J}_{j+1}) \langle \mathbf{s}_{j,(j+1)} \rangle^2\right) \end{aligned} \quad (5)$$

and the terms $\beta_j = (2\pi/\lambda)n_j(\lambda)d_j \sin(\mathbf{J}_j)$ define the phase of the outgoing wave and are responsible for the observed interference fringes. In the previous equation $\sigma_{j,(j+1)}$ represent the roughness between the “j” and the “j+ 1” layer.

The total matrix, which describes the system made of N layers, is obtained by multiplying all the characteristics matrices:

$$C(\mathbf{I}, \mathbf{J}) = \prod_{j=1}^N M^j(\mathbf{I}, \mathbf{J}) \quad (6)$$

The reflectivity is then given by:

$$R(Q) = \left(\frac{C_{2,1} \cdot C_{2,1}^*}{C_{1,1} \cdot C_{1,1}^*} \right) \quad (7)$$

From the above theoretical treatment it follows that the calculation of the reflectivity, given a refractive index profile, can always be calculated but the reverse process presents mathematical problems because all the quantities are imaginary and the phase is not known and, in general, is not measurable. Then the data are usually analyzed by performing a fitting procedure. The advantage of the given notation is that the contributions of the roughnesses between contiguous layers are easily included in the calculations.

Experimental Apparatus

Our aim is to measure the reflected intensity of an X-ray beam as a function of the exchanged momentum $Q = (4\pi/\lambda) \sin(\mathbf{J})$. From this relation follows that we can perform our measurements in two ways: either using a monochromatic incident radiation as a function of the incident angle \mathbf{J} , or having a white incident beam and employing an energy dispersive X-ray detector. We have chosen this second method and in Fig. 1 we show a layout of the instrument that is operational in our laboratory.

The instrument was specially designed to be able to measure reflectivities from liquid surfaces, so the scattering plane is vertical. The machine is mechanically very simple. It has two optical

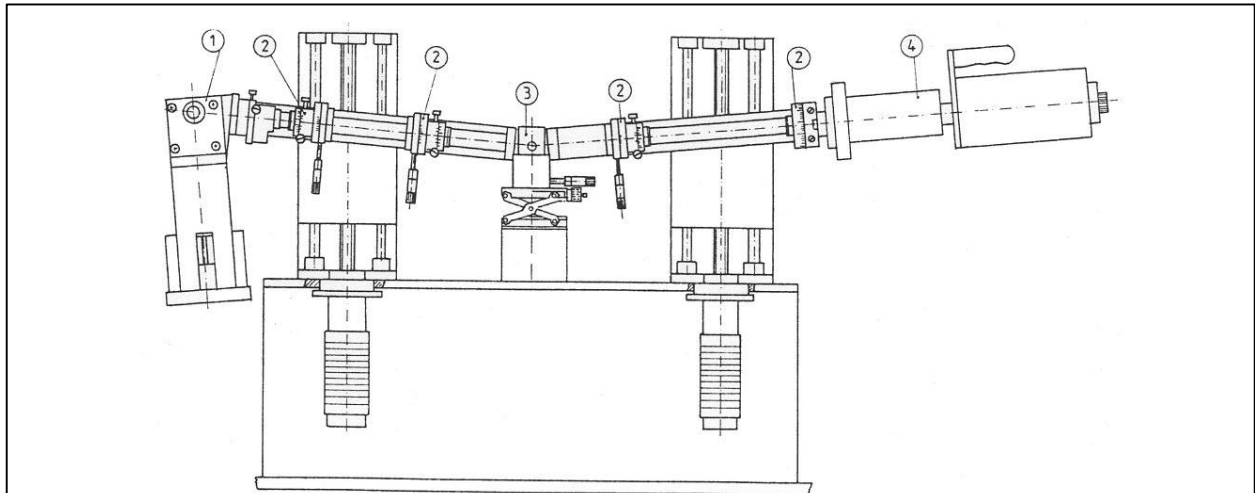


Fig. 1. Layout of the energy dispersive X-ray reflectometer built at ISM: 1) X-ray tube; 2) Collimating slits; 3) Sample position; 4) Single crystal solid-state energy sensitive detector. All the equipment is mounted on two optical benches pivoting around a single axis driven by two linear actuators.

benches pivoting around a single central axis. The X-ray tube is mounted on one arm while the detector is on the other one. The rotation axis is at the sample position. The white incident beam is produced by a standard X-ray tube and we have successfully employed Chromium and Tungsten as anode material. The two benches are moved by two linear actuators driven by stepping motors and the tangent of the angle is read by two linear encoders. Both the minimum step movement and the resolution of the encoders are of 1.µm leading to a minimum angle increment and reproducibility of 0.0004°. The incident and reflected beams are collimated by four slits made of blocks of tungsten 2 mm thick, whose minimum vertical apertures are 30.µm corresponding to an angular divergence of 0.004°.

The detection of the X-rays is performed by an EG&G acquisition system consisting of a planar HPGe solid state detector (6 mm in diameter), a 92X spectrum master which performs the amplification, the AD conversion and the multichannel analyzer functions and which is connected by an interface to an IBM computer running the Maestro software to visualize and to record the data. The energy resolution of the system is about 1% in all the used energy range being slightly better at high energies. The maximum counting rate is about 10000cps.

The measurement of the incident spectra is necessary to normalize the data. Its measurement is performed by putting the two arms in the straight position and collimating the beam to about 100x100 µm² with the first and fourth slits. In this way we are able to reduce the count rate to about 3000 cps with a current of 6 mA and a high voltage of 60 kV.

The first step in the data reduction is to correct for the transport function of the detector. In fact, inherent in the functioning of the Ge solid state detector, we have, for any incident X-ray photon of energy E, a finite probability of counting it at an energy (E-E_α) or (E-E_β) where E_α and E_β are the energies corresponding to the Ge-K_α and Ge-K_β transitions. These phenomena lead to echoes appearing in the spectrum. We measured the intensity of the echoes as a function of the incident energy by using the Bragg reflection from a Silicon single crystal. We are then able to remove them from the measured data numerically.

As a consequence of the λ^2 dependence of the refractive index a reflectivity curve always has higher intensity at low energies where the very intense fluorescence lines of the source are present. These can be strong enough to dominate the signal. We attenuate the low energy part of the spectra by inserting an appropriate filter (for instance a thin foil of aluminum or a slab of silicon). The resulting useful energy range goes from about 13 keV, just above the last I-line of the tungsten, to 55 keV. For many problems the Q range covered in one measurement is not sufficient to define all the structures of the reflectivity curve, then several runs at different angles are necessary. The normalization between two contiguous runs is obtained by integrating the overlap region.

Results

In this section we present typical measurements that can be performed with our X-ray reflectometer to show some of the advantages of using the energy dispersive technique. These are mainly related to the fixed angle geometry and to the high energy of the X-ray beam. Having everything fixed implies that the illumination of the sample does not change with respect to the exchanged momentum. Very small sample can thus be measured without suffering from the illumination problem. On the contrary, by using a monochromatic incident radiation and measuring as a function of the angle we must always be sure to intercept all of the beam. Consequently the sample has to be longer than the beam footprint which at low exchanged momentum can be several centimeters. With our instrument we were able to measure reflectivities from samples as small as 1 x3 mm². As an example of reflectivity curves we show in Fig. 2 the reflectivity from a Palladium film deposited onto a silica substrata. From this sample we can clearly observe the total reflection regime for exchanged momentum Q smaller than 0.068 Å⁻¹ and then the monotone decay as Q increases. The line is a fit to the data including 7% in the angular divergence of the incident beam and a surface roughness of 16Å. We report these data, which are not interesting in themselves, to show the effect of the absorption in the reflectivity curve. Using a white beam we may have a sample with an absorption edge in the energy range used in the experiment. In our case the useful energy range goes from 13 to 55 keV. Palladium has the

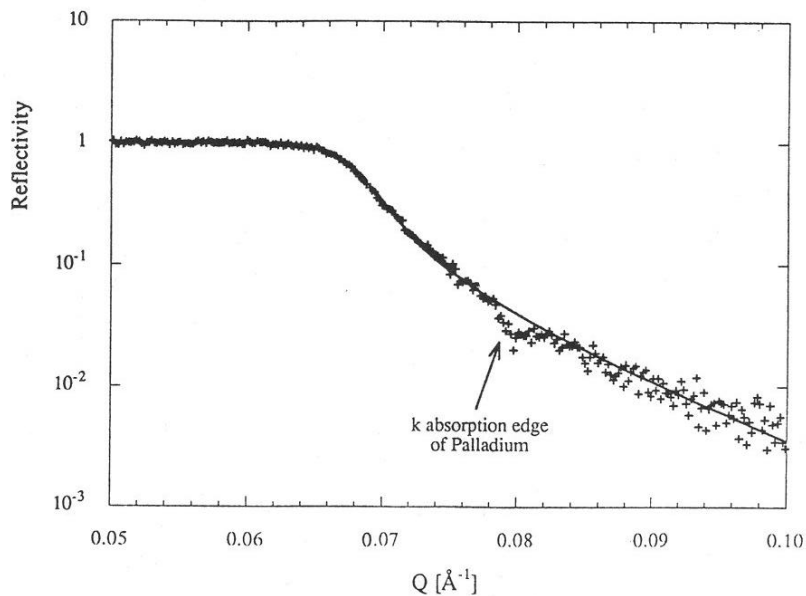


Fig. 2 X-ray reflectivity measurement from a Palladium film. The arrow indicates the position of the k absorption edge at 24.53 keV. The line is a fit to the data obtained neglecting the absorption coefficient in the refractive index expression.

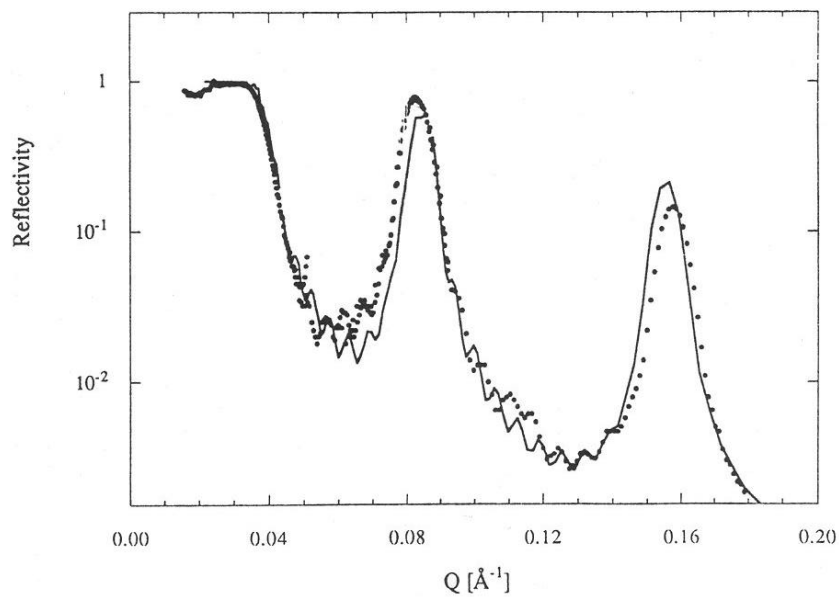


Fig. 3 X-ray reflectivity measurement from a Tungsten/Carbon multilayer. These data are the superposition of 4 runs at different incidence angles. Superlattice peaks are clearly visible and between them we can also observe the oscillation due to the whole film thickness. The line is a fit to the data.

K-absorption edge at 24.35 keV and its absorption linear coefficient changes by about two orders of magnitudes as measured in a trans-

mission experiment. However the effect of this big change in the linear absorption coefficient is very small in the reflectivity curve and it only pro-

duces a small dip in the measured data. The fit has been calculated without considering the imaginary part of the refractive index to make more evident the effect. The shape of the dip in the reflectivity curve is not similar to the usual shape of the linear absorption coefficient close to an absorption edge, because of the finite energy resolution of the detector, which is about 1%, corresponding to about 5 channels.

In Fig. 3 we report the reflectivity of a Tungsten-Carbon multilayer, made of a sequence of 11 bilayers, grown onto a Silicon single crystal. These data show the typical features of a reflectivity measurement from a superlattice: the presence of well defined peaks (the superlattice peaks) and, between them, small oscillations are clearly visible. From the position of the superlattice peaks we can immediately determine the dimension of the repeating unit. Moreover from the analysis of the their form factors we can also determine the thickness and the electronic density of all the layers inside the repeating unit, and the values of the roughness between two contiguous layers. These last parameters strongly affect the decay of the intensity of the high order superlattice peaks. The small oscillations among the superlattice peaks are instead due to the whole superlattice films grown on top of the silicon single crystal and their periodicity and intensity depends only on its thickness and average density of scattering. Unfortunately these oscillations are not very well defined because of the instrumental resolution in the exchanged momentum.

For this kind of instruments the resolution function depends on the beam divergence and on the electronic resolution. The divergence of either the incidence or reflected beams can be easily modified and controlled by varying the slit apertures and the X-Ray tube/Sample and Sample/Detector distances. Of course smaller is the beam divergence longer is the measuring time and, in principle, any angular resolution can be achieved. But the electronic resolution, which is about 1%, cannot be modified and this is the limiting value of the resolution in the exchanged momentum. This is why the oscillations among the superlattice peaks are not very visible, and is probably the main disadvantage of this technique. For the Tungsten/Carbon multilayer, which was about $2 \times 1 \text{ cm}^2$ the counting time for each measurement was about ten minutes for each angle. For

this sample we varied the slits aperture in order to maintain constant the resolution among the different runs.

The development of growing techniques under ultra high vacuum conditions allows the realization of superlattices with a control on the atomic scale of the thickness of each layer and the inter-diffusion between contiguous layers. These structures are of great interest for their novel characteristic physical properties and their possible technological applications. The use of the X-ray reflectivity measurements allows us to determine the average thicknesses of the layers of the sequence and the average dimension of the interface among the layers. We have also studied some heterojunctions of $\text{Si}_{1-x}\text{Ge}_x$ grown by molecular beam epitaxy (MBE) on Silicon. By these measurements we were able to determine the concentration of the Germanium with respect to the Silicon [11].

The other advantage of this technique is related to the strong penetration of hard X-rays. This allows us to study electronic density profiles at buried interface. For example we were able to measure the reflectivity from a gold film that was inside a water solution [12]. This may be used to study the nucleation of electrolytically deposited films.

Liquid-liquid interfaces are of fundamental importance in colloid and biological science but their structures are very difficult to measure. Because the difference in scattering length density between two liquids is in general very small (we do not consider the case where one of the liquid is Mercury) then the reflectivity must be measured at very small exchanged momentum Q . Moreover the meniscus that usually forms at the vessel walls may have dimension of few millimeters distorting the surface. For these reasons the sample has to be quite long, of the order of some centimeters. The system we chose to demonstrate the feasibility of the technique was made of water and cyclohexane, which is water insoluble. The scattering length densities of water and cyclohexane are $0.94 \times 10^{-5} \text{ \AA}^{-2}$ and $0.757 \times 10^{-5} \text{ \AA}^{-2}$ respectively. In order to increase the difference in the scattering length densities we added Calcium Chloride hexahydrate to the water at a concentration of approximately 7 moles per liter of water. The sample was contained in a Teflon vessel having 2 mm walls and it was 7 cm long. The white beam was measured by putting the arm in the straight posi-

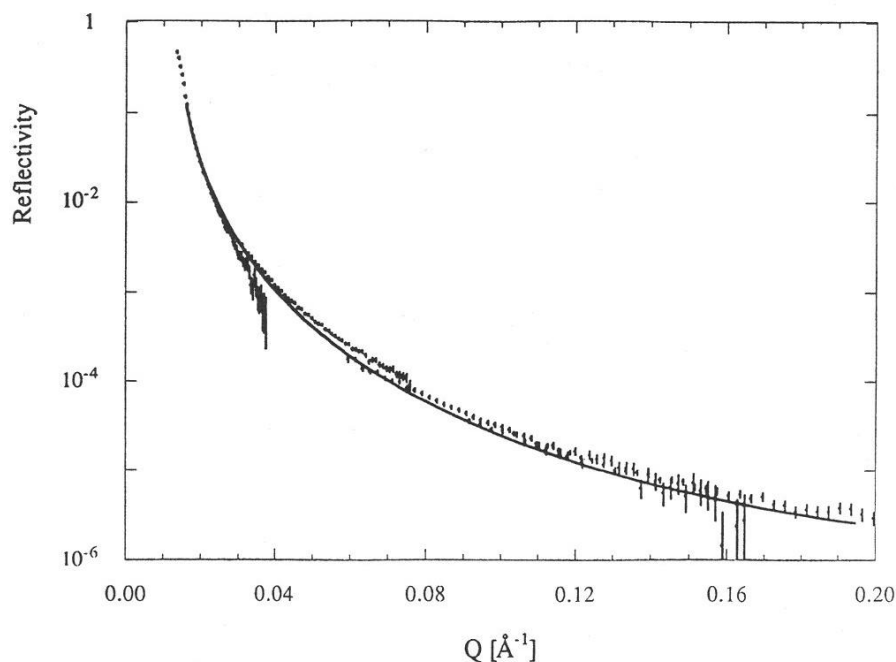


Fig. 4 X-ray reflectivity profile for Cyclohexane/ CaCl_2 water solution. In this case the X-ray beam travels through 7 cm of Cyclohexane. The line is a fit to the data. In this case the roughness between the two liquids is practically zero.

tion and having the beam through the Teflon walls and the cyclohexane to account for their adsorption. The transmission of the system was practically 1 for wavelength shorter than 0.4\AA ($\sim 30\text{keV}$) and it was falling down to 0.1 at 0.8\AA ($\sim 15\text{KeV}$). In Fig. 4 we report the reflectivity as a function of the exchanged momentum for four different angles: 0.044° , 0.085° , 0.193° and 0.297° . The interfacial roughness between the two liquids is practically zero. The interface between pure water and cyclohexane has instead a very different dimension. In this case the roughness at the interface is very large and we could not even observe the reflection of the X-rays. Measurements are planned to determine the dependence of this parameters with respect to the salt solution.

We then dissolved a surfactant in the water solution to determine the structure of the film which is supposed to form at the oil/solution interface. The X-ray reflectivity was substantially modified and by the fit procedure we were able to determine the average thickness of the film and the number of surfactant molecules per unit area [4].

Conclusions

In this paper we have shown that an energy

dispersive technique can be usefully employed to measure reflectivities at surfaces and interfaces. This method presents advantages with respect to the traditional measurements, which employ a monochromatic incident radiation, and allows us to measure reflectivity from very small samples and from buried interfaces. We have shown some application of these techniques and described some recent results. Moreover, because of the high penetration of high-energy X-ray beams, this technique can also be usefully employed in complicated sample environments and UHV chambers. Then it might be very useful for monitoring *in situ* the growth of film and superlattices.

The author would like to acknowledge Dr S. J. Roser for the helpful discussion in developing the instrument and to thank A. Ippoliti and F. Zuccaro for the technical support in building the apparatus.

References

- [1] L. G. Parrat, Phys. Rev., **95** (1954), 359.
- [2] R. M. Richardson, S. J. Roser, Langmuir, **7** (1991), 1458.
- [3] R. M. Richardson, S. J. Roser, Liquid Crystals, **2** (1987), 797.
- [4] S. J. Roser, R. Felici and A. Eaglesham, in press in

- Langmuir.
- [5] J. Lekner "Theory of reflection", Martinus Nijhoff Pub., Dordrecht (1987).
- [6] R. W. James, in "The Optical Principles of the Diffraction of X-rays", OX BOW Press, Woodbridge, Connecticut (1982).
- [7] L. Nevot and P. Croce, Phys. Appl., **15** (1980), 761.
- [8] J. Jacobson in "Progress in Optics", edited by E. Wolf, North-Holland Pub., Amsterdam, (1966).
- [9] M. Born and E. Wolf, in "Principles of Optics", Pergamon Press, Oxford (1970).
- [10] J. Penfold and R. K. Thomas, J. Phys. Condensed Matter, **2** (1990), 1369.
- [11] M. Mangiantini and R. Felici, in press in Vuoto.
- [12] S. J. Roser and R. Felici, unpublished data.